Geophys. J. Int. (2003) **154,** 754–766

The privilege as the cause of power distributions in geophysics

Zbigniew Czechowski

Institute of Geophysics, Polish Academy of Sciences, 01-452 *Warsaw, Księcia Janusza* 64, *Poland. E-mail: zczech@igf.edu.pl*

Accepted 2003 March 21. Received 2003 March 17; in original form 2002 January 18

SUMMARY

Power laws are known to be associated with dynamic systems residing near the critical point in the state space of the system. However, both models, that of phase transitions reached by the tuning parameter (for example, the percolation models) and SOC (self-organised critical) models, although leading to power-law relations, still do not explaining causes of their appearance.

In this contribution it is assumed that nature is random in its deep structure. The concept of the privilege, meaning the susceptibility of the state on to a change, is introduced. The model describing the privilege is analysed and applied to some known models: the Cantor set, the percolation theory and simple cellular automata. An adequate form of the privilege explains the appearance of the inverse-power distributions in many phenomena in geophysics. There is a relevance between the privilege concept and the results of a previous paper, in which the influence of the non-linearity of a model on the output behaviour was investigated.

Key words: Fractals, inverse-power distribution, non-linear transformation, percolation, self-organised criticality, stochastic models.

1 INTRODUCTION

We continue our previous attempt (Czechowski 2001) to understand the causes of the appearance of inverse-power distributions in nature. Strictly speaking, we assume that the structure of the medium, or the behaviour of intrinsic processes, is purely random on the lowest description levels, i.e. it may be characterized by purely random distributions such as: Poisson, exponential or Gaussian distributions. Next, we investigate, using some simple but general models, when and why the output distributions could be power-law -like.

Earthquakes are typical examples of phenomena that manifest power-law behaviour, and many models have been applied to the description of earthquakes. These include critical models, such as: percolation models (Vere-Jones 1976; Lomnitz-Adler 1988; Stauffer & Aharony 1992; Newman *et al.* 1994; Wu 1998; Turcotte *et al.* 2000), SOC models (Bak *et al.* 1988; Ito & Matsuzaki 1990; Sornette *et al.* 1990; Olami *et al.* 1992) or lately self-organized spinodal (SOS) models (Klein *et al.* 1997, 2000; Rundle *et al.* 1997, 1999, 2000). The models of first-order phase transitions which correspond to spinodal critical points in SOS have an additional advantage in that they could be described by a continuous approach. This is important, particularly in the context of the discussion given in Shaw & Rice (2000). We also claim that the discreteness is not the basic cause of the power-like behaviour. In our previous paper (Czechowski 2001) we have shown how the non-linearity of the continuous model leads to inverse-power distributions.

Here, we start from the concept that the cause of inverse-power (fractal) behaviour is some kind of privilege. It was shown (Czechowski 1993; Czechowski 1994, 1995) that the coagulation equation has an exponential solution for a constant fusion cross-section and has an inverse-power solution for the fusion cross-section proportional to the sum of sizes of two linking objects. The exponential distribution is an example of purely random distributions (a discussion on the purely random distributions is presented in Section 2 of the present paper), which originate randomly in processes without any interactions and independent of the past. On the other hand, the inverse-power distributions decrease much more slowly than random distributions (Fig. 1), and therefore, they are called long-tail distributions. The long tail means that greater events are more probable here than they would be for a purely random distribution. This means that greater events are in some way privileged in comparison with smaller events. If smaller and greater events have the same probability of evolution then the distribution function will be a Poisson one. This conclusion is a basis for further analysis in this paper.

In Section 3 we briefly present the dependence of the solutions of the coagulation equation on the form of the fusion cross-section. This help us to understand the physical source of the privilege.

We introduce (in Section 4) a simple model in which the privilege is taken into account and then we analyse the influence of the type of the privilege function on the form of the solutions. In Section 5 we present applications of the model to the formation of the Cantor set, to percolation models and to simple cellular automata. Section 6 shows how the privilege concept is linked to our previous paper (Czechowski 2001) in which we analysed the influence of the non-linearity of the model on the output distributions.

In the present paper, we will also use the designation 'inverse-power' for distributions that are not strictly inverse-power but only resemble them over some range of scales.

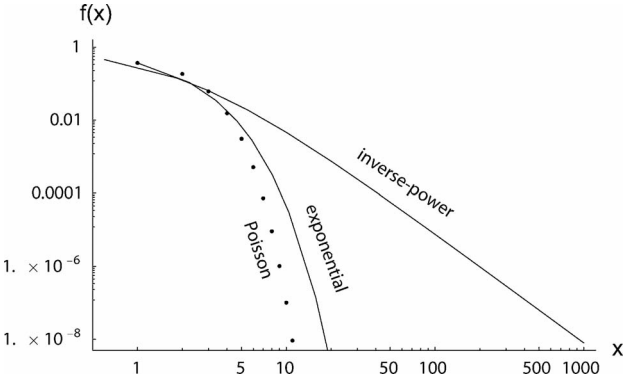

Figure 1. Graphs of the three distributions: Poisson, exponential and inverse-power, $f(x) = [x/(n-1)+1]^{-n}$. For each of them $f(0) = 1$.

2 PURELY RANDOM DISTRIBUTIONS

The Bernoulli trials scheme is a theoretical model describing n independent trials with a common binary outcome: a success with probability p and a failure with probability $q = 1 - p$. Let a random variable S_n denote the number of successes in n trials. Then the probability distribution function is given by the binomial distribution

$$P(S_n = k) = \binom{n}{k} p^k q^{n-k}. \tag{1}$$

On the other hand, a random variable T(the waiting time or lifetime) denoting the number of Bernoulli trials up to the first success has a geometrical distribution

$$P(T > m) = q^m. \tag{2}$$

For a partly continuous case, when the number of Bernoulli trials $n \to \infty$ and $p \to 0$ but $np \to \lambda$ remains constant, the binomial distribution converges to the Poisson distribution

$$P(S_\infty = k) = \frac{\lambda^k}{k!} \mathrm{e}^{-\lambda k} \tag{3}$$

and the geometrical distribution of waiting time converges to an exponential distribution,

$$P(T > t) = \mathrm{e}^{-\lambda t}. \tag{4}$$

The exponential (and the geometrical distribution in the discrete case) distribution has the Markov property, i.e. it does not depend on the past. Let $f(t)$ be the probability that the waiting time counted from 0 is longer then t, and let $f(t \mid t_1)$ be the conditional probability that the waiting time counted from 0 is longer than $t + t_1$ if it is known that during t_1 there were no successes. Then $f(t \mid t_1) = f(t + t_1)/f(t_1)$ is equal to $f(t)$ only when $f(t + t_1) = f(t)f(t_1)$. This condition is fulfilled only by the exponential (or geometrical) distribution.

For a continuous case, when $n \to \infty$, $p \to 0$ and $k \to \infty$ but

$$\frac{(k - np)^3}{(npq)^{3/2} n^{1/2}} \to 0 \tag{5}$$

the binomial distribution converges to the normal distribution:

$$\frac{1}{\sqrt{2\pi\sigma^2}} \mathrm{e}^{-\frac{1}{2}[(x-\mu)/\sigma]^2}, \tag{6}$$

where $np \to \mu$ (the mean) and $(npq)^{1/2} \to \sigma$ (the standard deviation).

However, the origin of both the Poisson and the normal distributions, is somewhat of a more noble birth than 'merely' as a limiting form of the binomial law. The Poisson law is based on three assumptions of the Poisson process which lead to recursive differential equations (see Section 4). Whereas assumptions of the Wiener process lead to the diffusion equation and its solution in the form of the normal (Gaussian) distribution.

Another way of the motivating why the distributions are purely random can be based on the maximum-entropy principle (see Montroll & Schlesinger 1983). A probabilistic interpretation of the thermodynamic entropy function is given by the formula

$$S = -\int f(x) \log f(x)\, dx, \tag{7}$$

where $f(x)$ is the distribution function. In the maximum-entropy formalism we seek the distribution function that maximizes the entropy subject to auxiliary conditions:

$$\int m_j(x) f(x)\, dx = c_i, \qquad i = 1, 2, \ldots, l, \tag{8}$$

where c_i are some known constants ($m_1(x) = 1$, $c_1 = 1$). For $m_i(x) = x^{i-1}$ the auxiliary conditions are i-moment conditions. By the method of Lagrange multipliers it could be shown that the distribution function that maximizes the entropy is given by the formula

$$f(r) = \exp(-1 - \lambda_1 - \lambda_2 m_2 - \cdots - \lambda_l m_l), \tag{9}$$

where the Lagrange multipliers λ_i are determined by the auxiliary conditions.

A microscopic interpretation of the maximum-entropy principle can be derived from the fact that S is a measure of the probability of the macroscopic state (see, e.g., Cercignani, chapter III, 9, 1975). This corresponds to the measure of information contained in the distribution function concerning the microscopic state, because a more probable state consists of a greater number of microscopic states with the same distribution function f and therefore such f gives very little information concerning the microscopic state.

By taking into account only some auxiliary conditions we can obtain different distribution functions which maximize the entropy function (e.g. the purely random distribution functions). If we know only the first moment $c_1 = 1$, then the distribution function is uniform:

$$f(x) = \begin{cases} \dfrac{1}{a} & x \in [0, a] \\ 0 & x \notin [0, a], \end{cases} \tag{10}$$

where we put $\lambda_1 = -1 + \log a$ and $\lambda_i = 0$ for $i = 2, 3, \ldots, l$.

When we assume additionally that we know the next moment c_2 then the exponential distribution

$$f(x) = b\exp(-bx), \qquad b = 1/c_2, \qquad x \geq 0, \tag{11}$$

maximizes the entropy, where we have set $\lambda_1 = -1 - \log b$, $\lambda_2 = b$, $m_2 = x$ and $\lambda_i = 0$ for $i = 3, 4, \ldots, l$.

The normal distribution

$$f(x) = \frac{1}{\sqrt{2\pi\sigma^2}} \mathrm{e}^{-\frac{1}{2}(x/\sigma)^2} \tag{12}$$

maximizes the entropy when we take into account the first moment $c_1 = 1$ and the third moment $c_3 = \sigma^2$, then: $\lambda_1 = -1 - \log\sqrt{2\pi\sigma^2}$, $\lambda_2 = 0$, $\lambda_3 = 1/(2\sigma^2)$, $m_3 = x^2$ and $\lambda_i = 0$ for $i = 4, 5, \ldots, l$.

3 THE COAGULATION EQUATION

The coagulation equation was applied to many different physical phenomena, for example: coagulation of aerosol particles; growth of

raindrops in meteorology; coagulation of planetesimals; and also to fusion of cracks in the earthquake preparation process. The integral (continuous) form of the equation is as follows:

$$\frac{\partial f}{\partial t} = \frac{1}{2}\int_0^y B(y', y-y')f(t,y')f(t,y-y')\,dy' - f(t,y)\int_0^\infty B(y,y')f(t,y')\,dy', \tag{13}$$

where $B(y, y')$ is the probability of fusion of two objects with sizes y and y', and $f(t, y)$ is the size distribution function of objects in time t. In was shown (Czechowski 1993) that for a constant coagulation coefficient $B(y, y')$ (there is no privilege—small and large objects fuse with the same rate) the solution of eq. (13) has the exponential form

$$f(t,y) \sim a(t)\mathrm{e}^{b(t)y}. \tag{14}$$

On the other hand, for $B(y, y') \sim y + y'$ (then the probability of fusion for larger objects is greater than for smaller objects—larger objects are privileged) we can mention the solution of the coagulation equation for planetesimals evolution (Safronov 1972):

$$f(t,y) \sim c(t)y^{-3/2} \tag{15}$$

for large y. The physical reason for such a form of $B(y, y')$ for gravitational bodies (planetesimals) is presented in Safronov (1972). However, it is evident that the gravitational cross-section increases with the growing body size. The example of planetesimals evolution is particularly valuable, because it directly joins the physical privilege (given by gravitational forces) with the coefficient $B(y, y')$ describing the rate of evolution of bodies.

Another application of the coagulation equation in geophysics was the problem of crack fusion (Czechowski 1991, 1993, 1997). It seems that for brittle materials, such as rocks, the fusion cross-section may also be given by $B(y, y') \sim y + y'$, because larger cracks induce greater stresses around its tips. Therefore, the process of fusion of numerous microcracks leads to the inverse-power distribution of crack sizes. Experimental investigations (e.g. Mogi 1962; Sholz 1968; Hirata 1987; Hirata *et al.* 1987) confirm this form of the distribution in rocks and ceramics. On the other hand, for ductile materials, such as metals, the exponential form of the crack size distribution was observed (see Curran *et al.* 1987), which suggests a weaker influence of tip stresses on to the crack fusion, probably due to the ductility.

The coagulation equation illustrates very well the role of the physical privilege in the creation of inverse-power distributions, but it has some weakness: it describes fusion processes only. Therefore, in the next section, we introduce a more general model which includes the privilege concept.

4 THE MODEL

Let us assume that the evolution of the system is given by the Markov process with continuous time and with discrete state space. Suppose that the probability that the system is at state N at time t is $p_N(t)$. Then for the system to be at state N at time $t + \Delta t$, either it was at state N at time t and no changes occurred in the subsequent short time interval $(t, t + \Delta t)$, or else it was at state $N - \Delta N$ at time t and a small change ΔN occurred in $(t, t + \Delta t)$. By choosing Δt sufficiently small we may ensure that the probability of greater change occurrence is negligible.

Let the probability of N changing to $N + \Delta N$ in $(t, t + \Delta t)$ be $B(N)\Delta t$; it follows that the probability of no change in $(t, t + \Delta t)$ is $1 - B(N)\Delta t$. Then we have

$$p_N(t+\Delta t) = p_N(t)[1 - B(N)\Delta t] + p_{N-\Delta N}(t)B(N-\Delta N)\Delta t. \tag{16}$$

On dividing both sides by Δt and as Δt approaches zero this becomes

$$\frac{dp_N(t)}{dt} = -B(N)p_N(t) + B(N-\Delta N)p_{N-\Delta N}(t) \tag{17}$$

for $N = N_0 + \Delta N, N_0 + 2\,\Delta N, \ldots$ (or for $\Delta N = 1$, $N = N_0 + 1$, $N_0 + 2, \ldots$). Since the set of states N is bounded from the bottom, we should introduce the additional equation for $N = N_0$. We put $B(N_0 - \Delta N) = 0$, therefore

$$\frac{dp_{N_0}(t)}{dt} = -B(N_0)p_{N_0}(t). \tag{18}$$

Such a boundary condition is called a 'natural' one (van Kampen 1987), it does not appear in the equations, so it is enough to solve the initial-value problem. Eq. (17) is the master equation for unistep processes with steps on the right only. This equation also describes the pure birth process.

The function $B(N)$, which denotes the probability of changing state N to state $N + \Delta N$, can be used for describing the privilege, when the privilege is the susceptibility of a given state on to a change. For example, if $B(N_2) > B(N_1)$ then we acknowledge that the state $N_2 (N_2 > N_1)$ is privileged.

Let us investigate the influence of various forms of function $B(N)$ on to a form of solution $p_N(t)$. We assume natural boundary conditions so we analyse the initial-value problem.

(a) Let $B(N) = \lambda =$ constant, i.e. all the states change with the same probability—there is no privilege. Then,

$$\frac{dp_N(t)}{dt} = \lambda[p_{N-1}(t) - p_N(t)], \qquad N = 1, 2, \ldots \tag{19}$$

$$\frac{dp_0(t)}{dt} = -\lambda p_0(t) \tag{20}$$

$$p_N(0) = \delta_{N,0}. \tag{21}$$

It is well known that the solution of eqs (16)–(18) is the Poisson distribution

$$p_N(t) = \frac{(\lambda t)^N}{N!}\mathrm{e}^{-\lambda t} \tag{22}$$

and that eq. (19) results from three assumptions of the Poisson law (see e.g. Stark & Woods 1986). The Poisson distribution (22) behaves like a wave travelling with velocity λ and undergoing dissipation. This form of the solution is in agreement with our main idea that the evolution without any imposed privilege leads to a purely random distribution.

(b) Let $B(N) = \lambda N$, i.e. the linear form of the privilege. Then,

$$\frac{dp_N(t)}{dt} = \lambda(N-1)p_{N-1}(t) - \lambda N p_N(t), \qquad N = 1, 2, \ldots \tag{23}$$

$$p_N(0) = \delta_{N,1}. \tag{24}$$

Eqs (23) are typical for pure birth processes where $p_N(t)$ is the probability that the population is of size N and λ is a rate of birth due to a single organism.

The solution of eqs (23) and (24) is the geometrical distribution:

$$p_N(t) = \mathrm{e}^{-\lambda t}(1 - \mathrm{e}^{-\lambda t})^{N-1}. \tag{25}$$

This distribution does not resemble a wave due to a large variation $V(t) = e^{\lambda t}(e^{\lambda t} - 1)$ about the mean $\mu(t) = e^{\lambda t}$. It is permanently J-shaped. We conclude that introducing a linear privilege $B(N) = \lambda N$ also leads to the purely random distribution, i.e. to the geometrical distribution. However, the geometrical distribution has a longer tail that the Poisson distribution.

(c) Let $B(N) = N^2$, a non-linear form of the privilege. Then,

$$\frac{dp_N(t)}{dt} = \lambda(N-1)^2 p_{N-1}(t) - \lambda N^2 p_N(t), \qquad N = 1, 2, \ldots \tag{26}$$

$$p_N(0) = \delta_{N,1}. \tag{27}$$

It is difficult to obtain a compact form of the solution of these recursive differential equations. However, we can show that for a sufficiently long time t the solution has a predominant term:

$$p_N(t) = \frac{2}{N(N+1)} e^{-\lambda t}[1 + a(N)e^{-3\lambda t} + b(N)e^{-8\lambda t} + \cdots]. \tag{28}$$

From numerical analysis it results that functions $a(N)$, $b(N)$, ... do not change the inverse-power form ($\sim N^{-2}$) of the solution. Figs 2(a)–(c) show solutions of eq. (26) with $B(N) = N^\alpha$ and the initial function $p_N(0) = e^{-N}$. We conclude that for $\alpha > 1$ and for sufficiently long times the solutions take inverse-power forms ($\sim N^{-\alpha}$) damped in time.

In some applications of the model it is useful to take into account boundary conditions. We assume the source of the lowest state N. To be more exact we put $p_1(t) =$ constant for every time t. This means that the transformation of the state $N = 1$ into higher states is balanced by the source. It should be noted that then the probability distribution $p_N(t)$ is not normalized to unity. Therefore, in this case, we will assume $p_N(t)$ to be the density of particles in state N.

Let us assume the three cases as before but with the boundary conditions.

(a′) Let $B(N) = \lambda$, then

$$\frac{dp_N(t)}{dt} = \lambda[p_{N-1}(t) - p_N(t)], \qquad N = 1, 2, \ldots \tag{29}$$

$$p_0(t) = c = \text{constant} \qquad t \geq 0 \tag{30}$$

$$p_N(0) = 0 \qquad N > 0. \tag{31}$$

It is easy to solve the recursive equations one after another and to deduce a solution in the form

$$p_N(t) = c - ce^{-\lambda t} \sum_{k=1}^{N} \frac{(\lambda t)^{k-1}}{(k-1)!}, \tag{32}$$

which has the Poisson tail.

(b′) However, for the linear function $B(N) = \lambda N$ and for the boundary condition $p_1(t) = c =$ constant the solution is

$$p_N(t) = \frac{c}{N}(1 - e^{-\lambda t})^N + c(1 - e^{-\lambda t})^{N-1} e^{-\lambda t} \tag{33}$$

and it tends asymptotically to the steady-state inverse-power solution $p^s{}_N = cN^{-1}$ for $t \to \infty$.

(c′) For a power form of $B(N) = \lambda N^\alpha$, $\alpha > 0$, the numerical solutions are presented in Figs 3(a)–(c). We observe similar behaviour of the solutions as in example (b′). Solutions converge to steady-state solutions $\sim N^{-\alpha}$. For slower increasing functions $B(N) \sim N^\alpha$ (smaller α), the evolution is slower and the time to attain the power-like form is longer.

We can conclude that by introducing the boundary condition of the source type we obtain steady-state solutions. These are inverse-power functions for $B(N) \sim N^\alpha$, for $\alpha > 0$. Therefore, even a very weak privilege given by $B(N) \sim N^\alpha$ with $0 < \alpha \ll 1$ leads to inverse-power solutions for a sufficiently long time t.

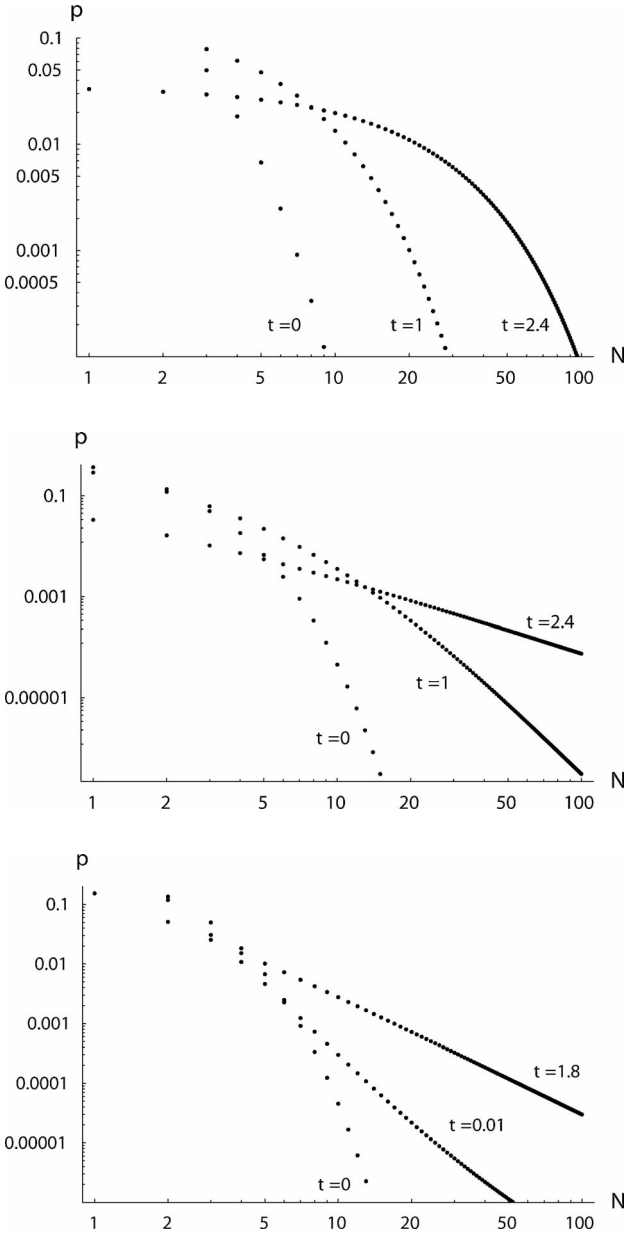

Figure 2. Solutions $p_N(t)$ of eq. (17) with the initial exponential function for some values of time: (a) $B(N) = N$. For each time t the exponential distribution is obtained. (b) $B(N) = N^{1.6}$. For $t = 2.4$ the power-like solution is obtained. (c) $B(N) = N^2$. For $t = 1.8$ we observe the power-like solution. For larger times the solutions in (b) and (c) do not change the power exponents.

5 APPLICATIONS OF THE MODEL

This section presents eight examples of application of the model introduced in the previous section. The first example is the geophysical model of the fault growth. We show what is the physical privilege in the process. The next examples concern some artificial, but very important, models.

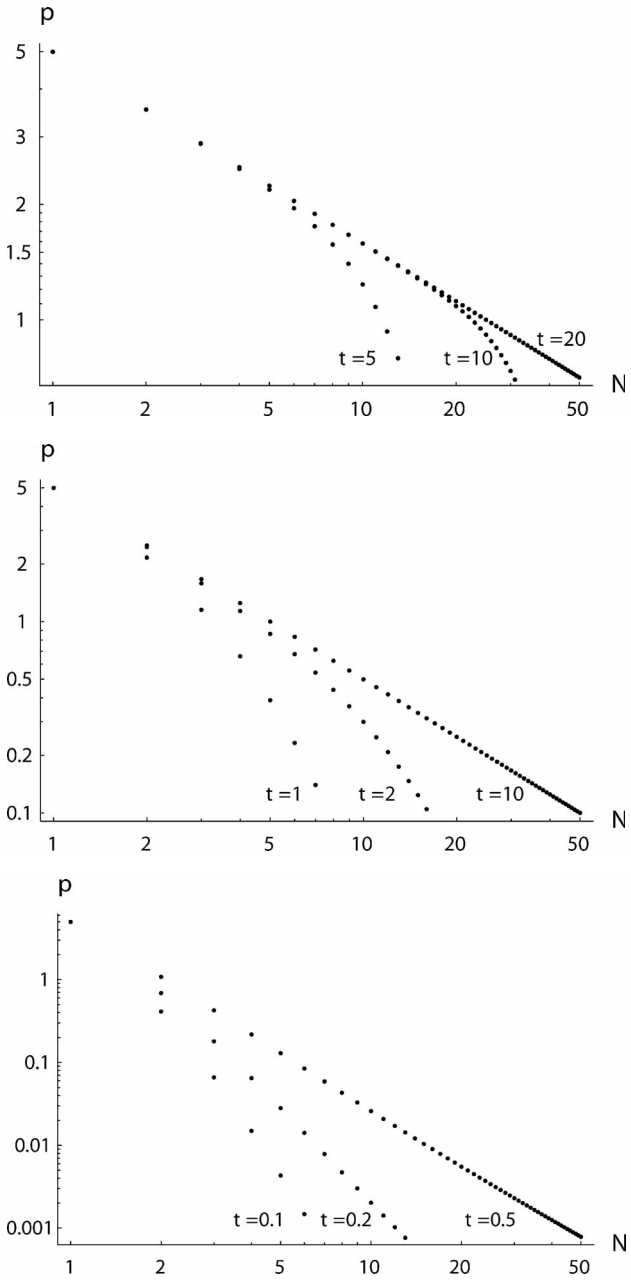

Figure 3. Solutions $p_N(t)$ of eq. (17) with the boundary condition of the source type for some values of time: (a) $B(N) = N^{1/2}$; (b) $B(N) = N$; (c) $B(N) = N^2$. For a power form of $B(N) \sim N^{\alpha}$, $\alpha > 0$ (privilege) an inverse-power form of solutions is observed for sufficiently long time t. These are steady-state solutions.

Fractals are typical objects that are described by the inverse-power distributions. So, according to our model, there should be a privilege during creation of the fractal. For clarity we investigate the simplest deterministic fractal—the Cantor set. We will show that the privilege is simply included in the deterministic recipe for the fractal.

Percolation models may be recognized as toy models but they are widely applied in many branches of science (e.g. they model phase transitions and lead to power dependences). It seems that in the percolation process, which is after all completely random, any privilege should be absent. However, in the following three examples (1-D, Bethe and 2-D percolation) we will prove, step by step, the existence of the privilege and explain its grounds.

Cellular automata are another form of toy model, but they describe interacting complex systems. They lead to self-organized criticality—the state which characterizes itself by the inverse-power distribution of avalanches. Cellular automata are typical computer models: the computer executes a simple rule many times. Therefore, seeking a privilege is a difficult task here. However, we will try to do this, step by step, in three last examples (1-D, Bethe and 2-D cellular automaton) by mapping the percolation clusters on to avalanches in cellular automata.

5.1 Fault evolution

We construct a model of a fault which includes the privilege concept. We follow Heimpel's (1996) model but we add a very important element, i.e. the time evolution of the model. A model fault is characterized as a surface composed of a large number of asperities, defined as small, discrete contact surfaces of finite strength. The rupture area grows by sequentially breaking asperities at the rupture boundary. Each asperity-breaking subevent adds a bit of area Δs to the rupture surface, so that, at a given state N of the process, the rupture area is $N\Delta s$. Assuming that this is a Markov process we obtain the equation for $p_N(t)$:

$$\frac{dp_N(t)}{dt} = -B(N)p_N(t) + B(N-1)p_{N-1}(t), \tag{34}$$

where $p_N(t)$ is the probability that the rupture is in state N at time t and $B(N)\Delta t$ is the probability that the rupture grows by Δs in Δt. Heimpel (1996) showed, assuming for the asperity failure probability the mixture of the Weibull densities, that the rupture growth probability $B(N)$ is given by the formula

$$B(N) = 1 - \frac{1}{1 + m(N)\,[\sigma(N)/\lambda]^{\gamma}}, \tag{35}$$

where $m(N)$ is the number of asperities along the rupture contour, $\sigma(N)$ is the stress, λ determines the degree of mixing of Weibull distributions and γ is the parameter of the Weibull distribution. The parameters $\sigma(N)$ and $m(N)$ are increasing functions of N, and therefore Heimpel (1996) put forward the formula

$$B(N) = 1 - \frac{1}{1 + (N/\Lambda)^{\Gamma}}, \tag{36}$$

where Γ and Λ are constants. Here, we assume $\Gamma = 1.5$ because $m(N)$ is proportional to the rupture perimeter $t(N) \sim N$ (such as for clusters in 2-D percolation, see Section 5) and $\sigma(N) \sim \sqrt{N}$ according to the stress intensity factor.

Fig. 4 shows solutions of eq. (34) with $B(N)$ given by (36) for different times. The solution evolves from the initial shape $\delta_{N,1}$ through exponential up to the power-like behaviour. The power exponent decreases: it is fitted to 1.51 for $t = 120$, 1.18 for $t = 200$, and 1.12 for $t = 300$. These values are consistent with observational data (see table 2 in Bonnet *et al.* 2001) where power exponents change from 1.76 to 3.2 for fault lengths, or from 0.88 to 1.6 for fault areas N. Therefore, according to the model, such a wide range of power exponents may be connected with different stages of time evolution of the fault. The deviation from the power-law behaviour for $N > 100$ (and $t = 200, 300$) results from too slow an increase of the function $B(N)$, which tends asymptotically to a constant value for large N. When $B(N)$ increases more slowly than a linear function, the solution of eq. (34) behaves as a travelling wave (see (a) in Section 4). For $N > 200$ (which is not presented in Fig. 4) the solution has a

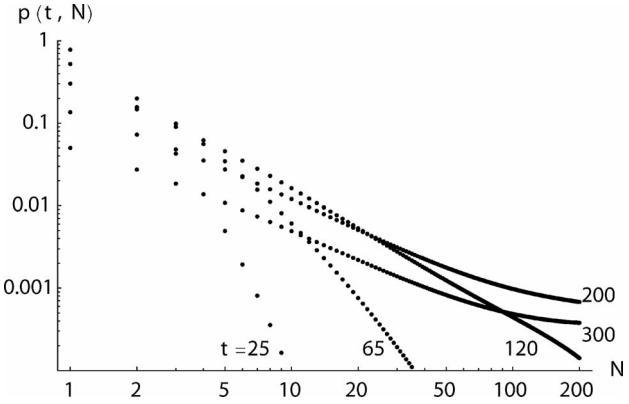

Figure 4. Solutions of eq. (34) with $B(N)$ given by eq. (36), where $\Gamma = 1.5$ and $\Lambda = 100$, for different times.

modal wave shape. However, the evolution of smaller faults leads to power-like distributions of fault sizes.

5.2 Growth of the Cantor set

The Cantor set is a well-known example of an uncountable set of points of measure zero. In fractal theory this set is considered to be a deterministic fractal with fractal dimension $D = \log 2/\log 3 = 0.630\,93$. The fractal dimension is defined as the power exponent at the function (box-counting method):

$$N_n = C r_n^{-D}, \tag{37}$$

where N_n is the number of boxes (rods in 1-D) of size r_n required to cover the fractal set. The box-counting method suggests the following definition of a fractal (see Turcotte 1992, p. 6): the fractal is a set of objects (fragments) with characteristic linear lengths r_n ($n = 1, 2, \ldots$), which fulfil relation (37). According to this definition, we can treat the Cantor set as a set of covering boxes with characteristic lengths r_n.

Let us derive the equation for the growth of the Cantor set. The set is composed of rods of lengths $r_k = 3^k$, $k = 0, 1, \ldots$. We start from the smallest fragments $r_0 = 1$. Let $n_k(t)$ be a number of rods of length r_k at time t. Then the number $n_k(t + \Delta t)$ at time $t + \Delta t$ is given by

$$n_k(t + \Delta t) = (1 - 2\lambda_{k-1}\Delta t)n_k(t) + \lambda_{k-1}n_{k-1}(t)\Delta t \tag{38}$$

and therefore

$$\frac{dn_k(t)}{dt} = \lambda_{k-1}n_{k-1}(t) - 2\lambda_{k-1}n_k(t), \tag{39}$$

where λ_{k-1} is the probability that a pair of neighbouring rods r_{k-1} produces a rod r_k. The factor of 2 in the second term on the right-hand side denotes that $\lambda_k = 2\,\lambda_{k-1}$ (because of the probability $\lambda_k = 1/$ (number of pairs of neighbouring rods) $= 1/(n_0 2^{-k-1})$) and it describes some privilege.

The problem of growth of the Cantor set corresponds to the boundary and the initial conditions:

$$n_0(t) = c = \text{constant} \qquad t \geq 0 \tag{40}$$

$$n_k(0) = 0 \qquad k > 0 \tag{41}$$

Then the solution of eq. (39) is

$$n_k(t) = \frac{c}{2^k}\left[1 - \mathrm{e}^{-2\lambda t}\sum_{j=1}^{k}\frac{(\lambda t)^{j-1}}{(j-1)!}2^{j-1}\right]. \tag{42}$$

For a long time t we obtain the geometrical distribution $n_k \sim 2^{-k}$. However, when we rescale the k-axis on to the r_k -axis we obtain an inverse-power distribution:

$$n_r(t) \sim r^{-\log 2/\log 3}, \tag{43}$$

where $r = 1, 3, 9, \ldots, 3^k, \ldots$.

In order to derive the equation for $n_r(t)$, where $r = 1, 2, \ldots$ (linear scale for r) we can put

$$\frac{dn_r(t)}{dt} = -B(r)n_r(t) + B(r-1)n_{r-1}(t) \tag{44}$$

and use the condition

$$B(r) = 2B\left(\frac{r}{3}\right), \tag{45}$$

where r corresponds to k, and $r/3$ corresponds to $k - 1$. Therefore, $B(r)$ has the form

$$B(r) = r^{-\log 2/\log 3} = r^{0.63093}, \tag{46}$$

which describes the privilege of greater rods.

From (c) of Section 4 we conclude that the solution of eq. (39) with the condition (40) converges for increasing time to a steady-state inverse-power solution $n_r \sim r^{-\log 2/\log 3}$.

5.3 Percolation models

The percolation theory (apart from 1-D percolation) is a simple model of second-order phase transitions which generally can be defined as follows: a system exhibits a qualitative change at one sharply defined parameter value, if the parameter is changed continuously. The behaviour of the systems close to the phase transition is usually described by power laws. For example, the cluster size distribution $n_s \sim s^{-\tau}$ for p near p_c, where s is a cluster size. The percolation model was also applied to a description of the fracture process in rocks and of earthquakes (Lomnitz-Adler 1985; Chelidze 1986; Wu 1998). Therefore, it would be very useful to explain, using the privilege concept, the appearance of an inverse-power distribution in percolation processes. We start from the simplest case; the 1-D percolation.

5.4 1-D percolation

Let us examine site percolation on an infinitely long linear chain, where lattice sites are placed at fixed distances. Each of these lattice sites is randomly occupied with probability p. Clusters in one dimension are chains of neighbouring occupied sites. Both left and right ends of the cluster must be empty. Thus, the perimeter t of the cluster is always 2, regardless of the cluster site. The number of clusters of size s (per lattice site) is

$$n_s = p^s(1-p)^2. \tag{47}$$

Let us imagine the percolation as an evolving process. We assume that p is an increasing variable which substitutes time. Let p increase to $p + \Delta p$(Δp denotes that one empty site becomes an occupied site). Then the probability of finding a cluster with size s is

$$n_s(p + \Delta p) = (1 - 2B)n_s(p) + s(1-p)Bn_{s-1}(p), \tag{48}$$

where B is the probability that a given empty site becomes occupied during Δp. The first term on the right-hand side denotes the probability that a cluster of size s does not increase during Δp, i.e. none of two empty sites on the perimeter becomes occupied. The second term on right-hand side denotes that, due to the growth of p to

$p + \Delta p$, there appears a cluster of size s from smaller clusters. There are s such possibilities. The first, when the cluster $s - 1$, which has no neighbour clusters, increases on one site. The second, when the cluster of size 1 is next to the cluster of size $s - 2$ and the empty site between them becomes occupied. The third, when the cluster of size 2 is next to the cluster of size $s - 3$ and the empty site between them becomes occupied, and so on. The probability of each of these possibilities is the same and is equal to the probability of finding an 's-cluster' composed of $s - 1$ occupied sites and one empty site within the 'cluster' (e.g. $n_{s-1}(p)\,(1-p)$). The probability B in each step of evolution is equal to $\Delta p/(1-p)$ because the probability of empty sites $(1-p)$ decreases in each step, Therefore, from eq. (48) we have

$$\frac{n_s(p+\Delta p) - n_s(p)}{\Delta p} = -\frac{2}{1-p} n_s(p) + s n_{s-1}(p) \tag{49}$$

and as Δp approaches zero this becomes

$$\frac{dn_s(p)}{dp} = -\frac{2}{1-p} n_s(p) + s n_{s-1}(p). \tag{50}$$

After easy transformations we obtain a more general form of eq. (17), i.e.

$$\frac{dn_s(p)}{dp} = -a(s,p) n_s(p) + a(s-1,p) n_{s-1}(p) + b(s,p) n_{s-1}(p), \tag{51}$$

where the coefficients

$$a(s,p) = \frac{2}{1-p} \tag{52}$$

$$b(s,p) = \frac{s(1-p) - 2}{1-p} \tag{53}$$

are functions of 'time' p.

Here, $a(s,p)$ does not depend on s so, according to (a) in Section 4, the solution should be the Poisson distribution. However, the influence of the gain term $b(s,p)\,n_{s-1}(p)$, which is positive for most of s (when p is away from $p_c = 1$), leads to the geometrical distribution which has a longer tail. The term $b(s,p)$ describes the privilege given by the fact that in the percolation problem the cluster of size s is created not only by growth of the cluster $s - 1$ on one site on their perimeter (which is described by $a(s-1,p)$), but also by linking of two neighbouring smaller clusters.

5.5 Bethe lattice

Besides the 1-D case, another case was solved exactly in the percolation theory. This is percolation on the Bethe lattice (see Stauffer & Aharony 1992). In spite of some shortcomings, the Bethe lattice has some advantages. It is often possible to derive analytical formulae for the properties of interest, and sometimes, surprisingly, the predictions of such formulae agree well with those for 3-D systems. Examples include conduction and permeability in a disordered Bethe lattice of coordination number 5, which estimates a cubic network (see Sahimi 1995, p. 188). The percolation problem on the Bethe lattice also corresponds to a branching process of crack formation (Vere-Jones 1976), which represents the problem of earthquake rupture.

We want to derive an equation of type (51) for this percolation problem. Let us note that the number of clusters of size s is given by

$$n_s(p) = g_s p^s (1-p)^{t(s)}, \tag{54}$$

where g_s is the number of different configurations for s-clusters on the Bethe lattice, $t(s) = (z-2)s + 2$ is the perimeter of s-clusters (t is not dependent on the configuration) and z is the coordination number (number of branches). For simplicity we assume $z = 3$.

As in the preceding section, we derive the form of $n_s(p + \Delta p)$:

$$n_s(p+\Delta p) = (1 - tB) n_s(p) + g_s p^{s-1} (1-p)(1-p)^t s B, \tag{55}$$

where the first term on the right-hand side denotes the probability that an s-cluster does not increase during Δp, i.e. none of t empty sites on the perimeter becomes occupied. The second term on the right-hand side describes the formation of s-cluster due to growth of the $(s-1)$-cluster by one occupied site or due to linking of two smaller clusters. It is equal to the number of 's-clusters' composed of $s - 1$ occupied sites and one empty site, times s possibilities of the choice of an empty site in this cluster, times B. This term is equal to

$$\frac{g_s}{g_{s-1}} (1-p)^2 s B n_{s-1}(p). \tag{56}$$

The ratio g_s/g_{s-1} can be determined using the known solution for the Bethe lattice, i.e. $n_s(p_c) \sim s^{-5/2}$ for large s (see Stauffer & Aharony 1992), where $p_c = 1/(z-1) = \frac{1}{2}$ is the percolation threshold for $z = 3$. Then, we can put

$$\frac{g_s}{g_{s-1}} = \frac{s^{-5/2}}{p_c^s (1-p_c)^{t(s)}} \frac{p_c^{s-1}(1-p_c)^{t(s-1)}}{(s-1)^{-5/2}} = 4\left(1 - \frac{1}{s}\right)^{5/2} \tag{57}$$

for large s. Therefore, the equation for $n_s(p)$ is

$$\frac{dn_s(p)}{dp} = -\frac{t(s)}{1-p} n_s(p) + \frac{t(s-1)}{1-p} n_{s-1}(p) + b(s,p) n_{s-1}(p), \tag{58}$$

where

$$b(s,p) = \frac{s[4(1-1/s)^{5/2}(1-p)^2 - 1] - 1}{1-p}. \tag{59}$$

It is easy to show that for p away from p_c (and $p < p_c$) the coefficient $b(s,p)$ is positive for large s.

5.6 2-D percolation

The 2-D case is much more complex than the percolation on the Bethe lattice because s-clusters have a few or more different perimeters. Therefore, the number of s-clusters per lattice site is given by the sum over all possible perimeters t (see Stauffer & Aharony 1992):

$$n_s(p) = \sum_{t(s)} g_{st} p^s (1-p)^{t(s)} \equiv \sum_t n_{st}(p), \tag{60}$$

where g_{st} is the number of different configurations of s-clusters with perimeter t. There seems to be no exact solutions for general t and s available at present, and this is why the percolation cluster problem has not yet been solved exactly.

However, it is easy (see eq. 55) to derive the equation for the number of s-clusters with a given perimeter t; i.e. for $n_{st}(p + \Delta p)$:

$$n_{st}(p+\Delta p) = (1 - tB) n_{st}(p) + g_{st} p^{s-1} (1-p)(1-p)^t s B. \tag{61}$$

Therefore,

$$\frac{dn_{st}(p)}{dp} = \left[-\frac{t(s)}{1-p} + \frac{s}{p}\right] n_{st}(p) \tag{62}$$

and after summing over t:

$$\frac{dn_s(p)}{dp} = \left[-\frac{\bar{t}(s)}{1-p} + \frac{s}{p}\right] n_s(p), \tag{63}$$

where we have introduced the average perimeter $\bar{t}(s) = \sum_t t n_{st}(p)/$

$n_s(p)$. In order to obtain the formula for $b(s, p)$ (such as for the Bethe lattice), we use the two results of the percolation theory (see Stauffer & Aharony 1992):

$$n_s(p) \sim s^{-\tau} \exp\left[-s(p_c - p)^w\right] \tag{64}$$

and

$$\bar{t}(s, p) \sim s(1-p)\left[\frac{1}{p} - w(p_c - p)^{w-1}\right], \tag{65}$$

which are valid for $p < p_c$ and for large s. Then,

$$b(s, p) = \frac{s}{p}\frac{n_s(p)}{n_{s-1}(p)} - \frac{\bar{t}(s-1, p)}{1-p} \tag{66}$$

$$= \frac{s}{p}\left(1 - \frac{1}{s}\right)^{\tau} \exp\left[-(pc - p)^w\right] - \frac{s-1}{p}\left[1 - wp(p_c - p)^{w-1}\right], \tag{67}$$

where $w = 91/36$ and $\tau = 187/91$ for $p \to p_c$ and $\tau \to 1$ for $p \to 0$. The equation for $n_s(p)$ has the form

$$\frac{dn_s(p)}{dp} = -\frac{\bar{t}(s)}{1-p}n_s(p) + \frac{\bar{t}(s-1)}{1-p}n_{s-1}(p) + b(s, p)n_{s-1}(p). \tag{68}$$

The term $b(s, p)$ has a similar behaviour as an adequate term for the Bethe and 1-D lattice and describes the same privilege.

We have shown that the percolation process can be described by the master equation modified by the additional term $b(s, p)n_{s-1}(p)$. The function $B(N) = t(s)/(1-p)$ describing the privilege is given by the perimeter $t(s)$ (or the average perimeter) of the s-cluster. The longer perimeter really means greater probability of growth of the s-cluster on one site, because each of $t(s)$ empty sites on the perimeter may become the occupied site when p increases to $p + \Delta p$. The perimeter $t(s) = 2$ for 1-D percolation and $t(s) \sim s$ for the Bethe percolation and for 2-D percolation. Therefore, if we omit the term $b(s, p)n_{s-1}(p)$, we obtain (see Section 4) the Poisson distribution for 1-D percolation and the geometrical distribution for the Bethe and 2-D percolation.

However, in the percolation process there is an additional gain term of s-clusters. The s-clusters can be created not only by growth of the $(s-1)$ -cluster on one site (which is described by the term $t(s-1)n_{s-1}(p)/(1-p)$), but also by linking of neighbouring smaller clusters when a site on the intersection of their perimeters will become occupied. This is included in the additional term $b(s, p)n_{s-1}(p)$. The function $b(s, p)$ has a similar behaviour for the three types of percolation: it is an increasing (linear) function of s, it is positive for $p < p_c$ (and for sufficiently big s) and it is negative for $p = p_c$ (for all s). The additional privilege (when $b(s, p)$ is positive) leads to the geometrical distribution for 1-D percolation (which has a longer tail then the Poisson distribution), and to the power-like distribution for the Bethe percolation and 2-D percolation. Therefore, we have shown how the privilege concept explains the appearance of inverse-power distributions in percolation models.

5.7 Cellular automata

The next important class of models that lead to fractal statistics are SOC models. We consider only the simplest cellular automata model on a 1-D grid, the Bethe grid and a 2-D square grid, in analogy to the percolation problems. In the percolation theory, greater clusters are privileged because they have longer perimeters and, additionally, they have more ways (due to the factor of g_s or g_{st}) of creating greater clusters by linking clusters, than smaller clusters. The avalanches in cellular automata define some 'potential' dynamic clusters; the group of neighbouring boxes that will become unstable in the event, if one selected box becomes unstable. Therefore, we will treat such a 'potential' cluster in a similar way to the percolation cluster (in the same geometry) and adequate privilege arguments should be valid.

5.8 1-D cellular automata

Consider a linear grid of boxes. There are three states for each box: 0, 1 and 2. Use the following rules: when a box has two particles (state 2) it is unstable and they are redistributed to the two adjacent boxes, and so on. Particles are lost from the ends of the linear grid. The size of a multiple event (avalanche) is the number of boxes that become unstable in the event.

In some sense the cellular automata resembles the percolation model, but here the multiple events (avalanches) are not static objects as clusters (of occupied sites) in percolation. They are dynamic objects composed of neighbouring boxes, which 'potentially' could take part in the multiple event. We call them the 'potential' clusters.

The 'potential' clusters in 1-D cellular automata are simply the clusters of adjacent boxes in state 1. This means that they are exactly the same as clusters of occupied sites in the 1-D percolation model.

5.9 Bethe lattice cellular automata

Consider the Bethe lattice with coordination number z. Then each site can be at $z + 1$ states $(0, 1, \ldots, z)$. The state z is unstable: z particles are redistributed to the z adjacent sites. The 'potential' clusters here are the clusters of neighbouring sites of state $z - 1$. Therefore, the 'potential' clusters can be identified with clusters of occupied sites in percolation on the Bethe lattice. Eq. (58) for the evolution of the number of clusters may be used here if the 'time' Δp is to be replaced by the probability that the state i of the site changes on to the state $i + 1$ $(i = 0, 1, \ldots, z - 1)$ and then we put $B =$ (probability that the state $z - 2$ of a given site changes on to the state $z - 1$)/(number of sites with the states $< z - 1$).

5.10 2-D Bak–Tang–Wiesenfeld cellular automaton

We consider a square grid of n boxes. Particles are added to and lost from the grid using the following procedure: a particle is randomly added to one of the boxes; when a box has four particles (state 4) it is unstable and the four particles are redistributed to the four adjacent boxes, or are partly lost from the grid when we consider edge boxes or corner boxes.

In 2-D cellular automata, 'potential' clusters are much more complex. They can be composed not only of boxes of state 3, but also of boxes of states 2, 1 and even 0 arranged in a 'specific configuration'. It seems that, as in the 2-D percolation, the perimeter of the 'potential' cluster is (on average) proportional to its size. Therefore, here we can use some conclusions concerning the privilege from 2-D percolation, although we cannot propose an equation of type (68) for the evolution of 'potential' clusters.

The 'specific configurations' of boxes in different states on the grid in 2-D cellular automata around the critical state appear after the complex process of activity of cellular automata, i.e. after many avalanches which rearrange the system.

In order to demonstrate that the privilege at the cellular automaton may have similar roots as the privilege for percolation models we should show that the 'specific configurations', which are created by the cellular automaton, are (statistically) similar to random configurations (because the percolation process is random) in the sense that they both lead to similar inverse-power distributions.

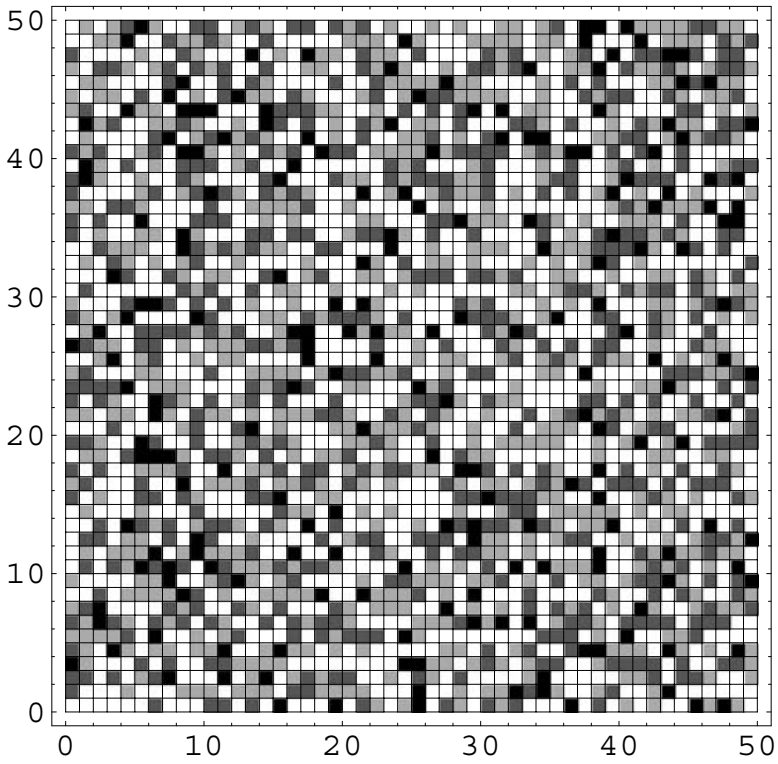

Figure 5. A grid created by SOC. White boxes denote state 3, black state 0.

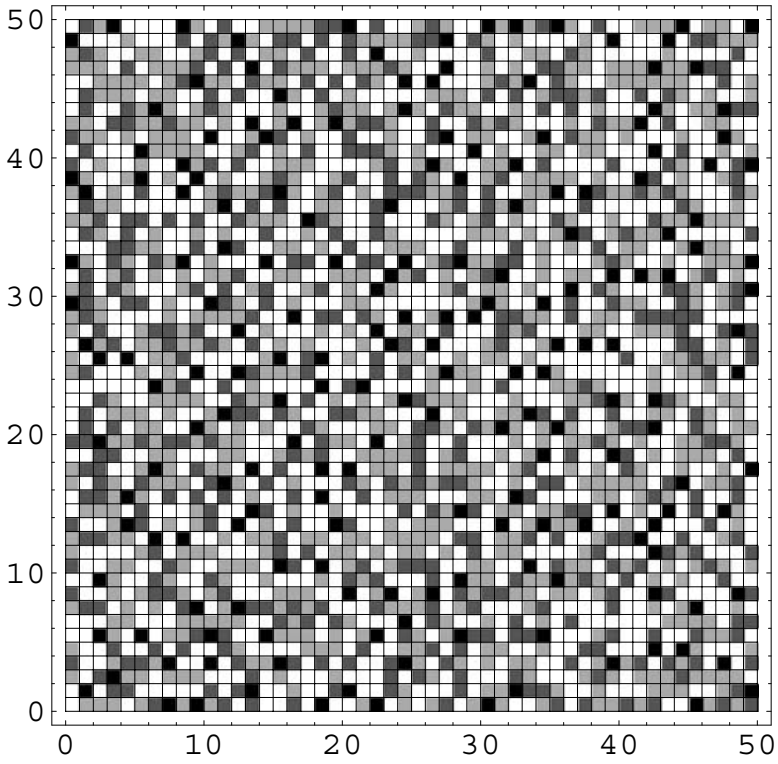

Figure 6. A randomly created grid. White boxes denote state 3, black state 0.

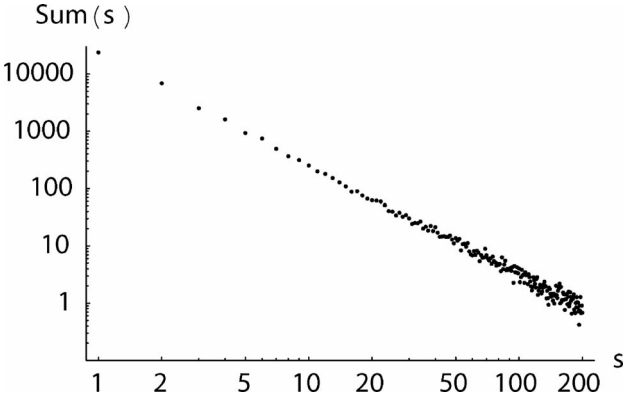

Figure 7. Graph of the Sum$(s) = \sum_i n_s^{(i)}/s$ which illustrates the avalanche size distribution obtained from the grid created by SOC. The fitted power exponent is 1.955 99.

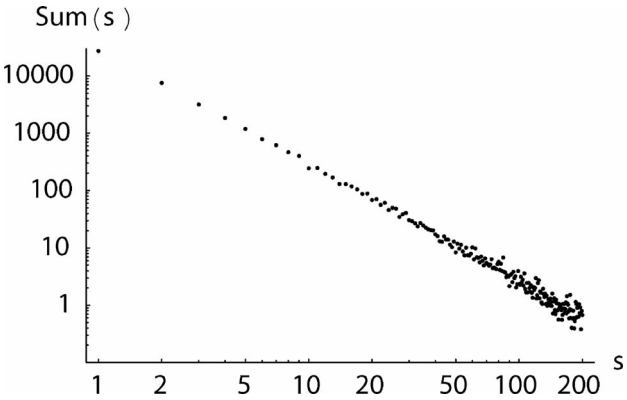

Figure 8. Graph of the Sum$(s) = \sum_i n_s^{(i)}/s$ which illustrates the avalanche size distribution obtained from randomly created grid. The fitted power exponent is 1.956 25.

To this end, we analyse two series of computer simulations. In the first, the critical distribution of states of boxes is created by itself during the self-organization process of the cellular automata. Next, the critical state of the grid is analysed by investigation of avalanches initiated by each box of state 3 (one after another; after each step (avalanche) the state of the grid was restored to the initial state). Fig. 7 presents the sum, $\sum_i n_s^{(i)}/s$ over the number i of simulations, of avalanches with size s, divided by their size (because each of the boxes with state 3 from the 'potential' cluster can trigger the avalanche). The inverse-power function with the power exponent 1.955 99 is fitted (least-squares fit) to the results.

In the second series, particles are randomly added to boxes omitting the boxes of state 3. This procedure is executed as long as the number of boxes of state 3, 2, 1, 0 is the same as in the critical state of the grid in the first series of simulations. Next, we investigate the avalanches initiated by each box of state 3 (one after another; after each step (avalanche) the state of the grid was restored to the initial state). Fig. 8 shows an adequate distribution of the sum, $\sum_i n_s^{(i)}/s$. Here, the power exponent is 1.956 25.

We conclude that although distributions of states on the grids look different in the two series of simulations (Figs 5 and 6), however, the exponents are practically the same.

It follows that although interactions between boxes in cellular automata may lead to some 'specific configurations' of states, however, the random state of the grid gives similar statistics. This simply means that the privilege (which has similar roots to the privilege for percolation models) of the cellular automaton, which results from a random distribution of cell states, is a good approximation to the real privilege hidden in Bak–Tang–Wiesenfeld cellular automaton activity.

6 RELEVANCE OF THE PRIVILEGE APPROACH TO THE NON-LINEARITY APPROACH

In our previous paper (Czechowski 2001) we have shown how a non-linearity of the model transforms an input purely random distribution on to the inverse-power output. It is interesting to find the relevance between the privilege which is given by the form of $B(N)$ in eq. (17) and the non-linearity of the model from the previous paper.

The continuous version (discrete $N\rightarrow$ continuous y) of the master equation (eq. 17) is the Fokker–Planck equation:

$$\frac{\partial f(t,y)}{\partial t} + \frac{\partial [f(t,y)B(y)]}{\partial y} - \frac{1}{2}\frac{\partial^2 [f(t,y)B(y)]}{\partial y^2} = 0 \tag{69}$$

$$f(0,y) = \mathrm{e}^{-y}. \tag{70}$$

Figs 9(a)–(c) present solutions of eq. (69) for the initial-value problem, $f(0,y) = \mathrm{e}^{-y}$, and for $B(N) = y^{\alpha}$, $\alpha = 1, 2, 3$. The behaviour of the solutions is analogous to that in the discrete model, i.e. for $\alpha > 1$ we obtain the inverse-power form of the solution.

The connection between the Fokker–Planck and the Ito equation may be found using the Ito formula (see, e.g., Gardiner 1985, ch. 4). Then, the Ito equation, which corresponds to eq. (69), has the form:

$$dy(t) = B(y)\,dt + \sqrt{B(y)}\,dW(t), \tag{71}$$

where $W(t)$ is the Wiener process. The Ito equation corresponds to the Langevine equation. For the Ito interpretation we have

$$\frac{dy}{dt} = B(y) + \sqrt{B(y)}\xi(t). \tag{72}$$

The Langevine equation is an example of a random differential equation with a random force given by the white noise $\xi(t)$ and modified by the function of the state, $\sqrt{B(y)}$. The equation can be analysed with a deterministic or stochastic initial function $y(0)$.

When we omit the random force term (diffusion term) in eq. (72) then we obtain a simple random initial problem which was analysed in Czechowski (2001):

$$\frac{dy}{dt} = B(y) \tag{73}$$

$$y(0) = x, \tag{74}$$

where x is a random variable with exponential probability density $f(x) = \mathrm{e}^{-x}$. It is shown in Czechowski (2001) that for a linear form of $B(y) \sim y$, the distribution function of $y(t, x)$ also has an exponential form, but for non-linear $B(y) = cy^{\alpha}$ and for $\alpha > 1$ the solution of eq. (73) has a power-like distribution (for sufficiently large y):

$$f(t,y) = \frac{1}{[1 + c(\alpha-1)y^{\alpha-1}t]^{\alpha/(\alpha-1)}} \times \exp\left\{\frac{-y}{[1 + c(\alpha-1)y^{\alpha-1}t]^{1/(\alpha-1)}}\right\} \tag{75}$$

while the solution is given by

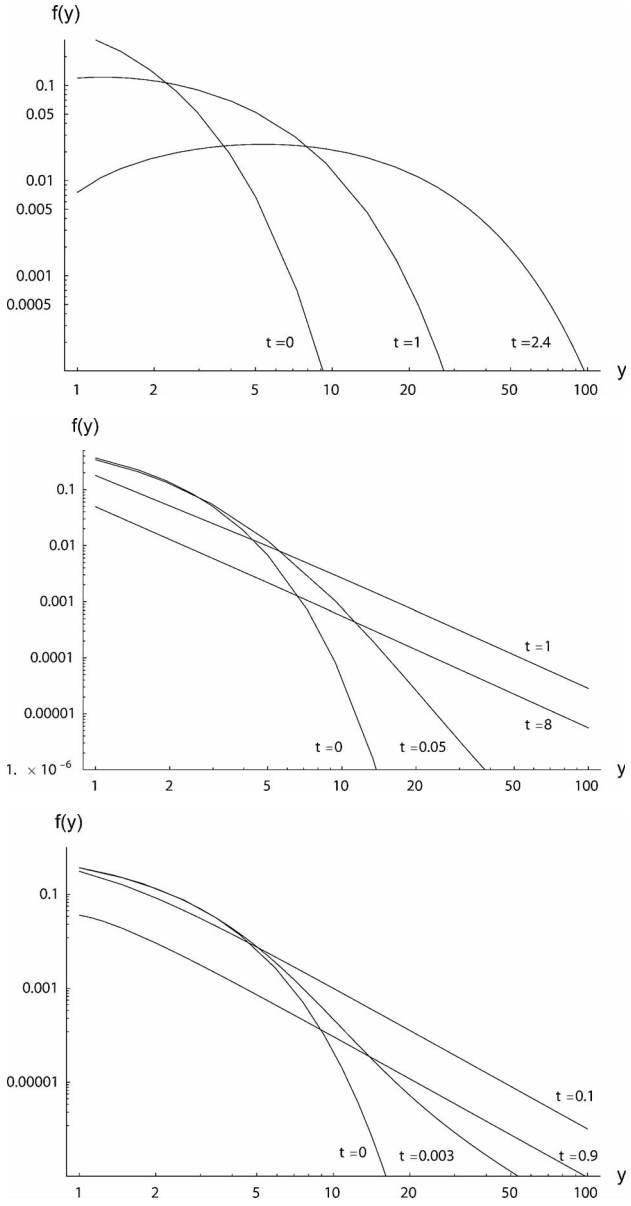

Figure 9. Solutions of the Fokker–Planck equation for some values of time: (a) $B(y) = y$ (b) $B(y) = y^2$ (c) $B(y) = y^3$. For larger values of time the solutions in (b) and (c) do not change the power exponents.

$$y(t, x) = \frac{x}{[1 - c(\alpha - 1)x^{\alpha-1}t]^{1/(\alpha-1)}}. \tag{76}$$

The cause of such a substantial change of the distribution function from exponential to inverse-power is the strong non-linearity in the dependence of $y(t, x)$ on the initial random value x (this problem was investigated in Czechowski 2001). From eq. (76), for $\alpha > 1$ the solution $y(t, x)$ goes to infinity along the vertical asymptote. In this way we have found agreement between the problem (73), (74) and the solutions of the Fokker–Planck equation (or the master equation) when we take into account the initial problem.

Additionally, the Liouville theorem proves that the distribution function $f(t, y)$ of the solution $y(t, x)$ satisfies the Liouville equation:

$$\frac{\partial f(t, y)}{\partial t} + \frac{\partial [f(t, y)B(y)]}{\partial y} = 0 \tag{77}$$

$$f(0, y) = \mathrm{e}^{-y}. \tag{78}$$

Of course, this equation may be interpreted as the Fokker–Planck equation without the diffusion term. This is in agreement with the assumption given before eq. (73) that we omit the random force term. Therefore, regarding the diffusion term we return to the Fokker–Planck equation, bringing to an end our circle of relevance.

The non-linear form of $B(y) = y^\alpha$ in eq. (73) determines the inverse-power form ($\sim y^{-\alpha}$) of the distribution function $f(t, y)$, and similarly, the non-linear form of the privilege function $B(y) = y^\alpha$ determines the inverse-power form ($\sim y^{-\alpha}$, see Fig. 9) of the solution $f(t, y)$ of the Fokker–Planck equation.

In this way we have shown, on one hand, how the privilege is described by non-linear functions and, on the other hand, how the non-linearities in many models (see Czechowski 2001) may gain a physical description given by the privilege concept.

7 CONCLUSIONS

In order to take into account the privilege, we have introduced the model based on the master equation for the pure birth processes. According to the form of the function $B(N)$, which describes the privilege, we have obtained various forms of solutions. For natural boundary conditions, inverse-power solutions appeared for $B(N) = N^\alpha$ when $\alpha > 1$. However, when we introduced the boundary conditions of the source type, we obtained inverse-power solutions (steady-state solutions) for $\alpha > 0$ (i.e. even for a very weak privilege).

The model is quite general. It describes any Markov processes in which discrete states of the system can be arranged in a sequence (and there is no return to preceding states). For a continuous space of states, the model resolves itself to the Fokker–Planck equation but it retains its own behaviour.

It should be noted that there is a relevance between the present model and our previous non-linear approach (Czechowski 2001). The Fokker–Planck equation corresponds to an adequate Ito equation and a Langevine equation which is an example of a random differential equation. If in the non-linear approach we choose as the model, $y = g(x)$, the random initial problem (73) and (74) then, according to the Liouville theorem, we find the linking between the two approaches. In this way we have shown, on the one hand, how the privilege is described by non-linear functions and, on the other hand, how the non-linearities in many models may gain a physical description given by the privilege concept.

We have applied our model to a simple geophysical model of the fault evolution and to the formation process of: the Cantor set, clusters in percolation (1-D percolation, Bethe-lattice percolation and 2-D percolation) and 'potential' clusters in cellular automata. It appears that a weak privilege $B(N) = N^{0.63093}$ is sufficient for creation of a fractal (the Cantor set) because the boundary condition of the source type was taken into account. On the other hand, the natural boundary condition must be used for the percolation problem. Then, the linear privilege (for the Bethe lattice and 2-D lattice) is too weak to create inverse-power distributions (it leads to the geometrical distribution). We have shown that the inverse-power form of the number of s-clusters is connected with the fact that clusters

are not isolated on the grid and so larger clusters can form by linking smaller clusters.

We have identified the creation of avalanches in cellular automata with the creation of clusters in percolation. This is quite obvious for the 1-D problem or for the Bethe lattice; however, for the 2-D lattice this is a very difficult problem, because 'potential' clusters are composed of sites of different states. However, we have shown that the critical state of the whole lattice need not be created by the specific form of cellular automata activity, but it could be formed in a purely random way (such as in the percolation problem). Then, distributions of avalanches are practically the same. This means that the 'potential' dynamic clusters (avalanches) could be treated like the percolation clusters.

It has not been our goal to give an alternative description of percolation processes or cellular automata. We have intended to extract and to understand the hidden privilege, which, according to our hypothesis, is responsible for inverse-power distributions. It has been especially important due to the fact that the percolation is a simple model of phase transitions and cellular automata represent a simple description of complex interacting systems. It was know that, apart of non-linearities (and connected with them chaos and strange attractors), phase transitions and interactions were considered to be responsible for the appearance of inverse-power distributions. It seems that the enclosing of these three different causes into a unified description (by the privilege) brings some order to our knowledge in this field.

The connection of these approaches with other types of equations, such as the Fokker–Planck, Ito, Langevine and Liouville equations, increases the universality of the explanation. The model may be used for a description of many phenomena in physics, geophysics, biology and economics. We hope that the extraction of the real privilege will be possible and will explain the appearance of fractal distributions in the phenomena.

The paper presents an approach which joins together discrete models, continuum models, hierarchical models and critical models, and it shows the influence of the privilege on the output distributions.

ACKNOWLEDGMENTS

I would like to thank the anonymous reviewers for their comments which helped me to improve the clarity of the manuscript. The work was supported by KBN grant no 6 P04D 039 15.

REFERENCES

Bak, P., Tang, C. & Wiesenfeld, K., 1988. Self-organized criticality, *Phys. Rev.,* A, **38,** 364–374.

Bonnet, E., Bour, O., Odling, N.E., Davy, P., Main, I., Cowie, P. & Berkowitz, B., 2001. Scaling of fracture systems in geological media, *Rev. Geophys.,* **39,** 347–383.

Cercignani, C., 1975. *Theory and Application of the Boltzmann Equation,* Scottish Academic Press, Edinburgh.

Chelidze, T.L., 1986. Percolation theory as a tool for imitation of fracture process in rocks, *Pageophys.,* **124,** 731–748.

Curran, D.R., Seaman, L. & Shockey, D.A., Dynamic failure of solids, *Phys. Today,* **1,** 46–55.

Czechowski, Z., 1993. A kinetic model of nucleation, propagation and fusion of cracks, *J. Phys. Earth,* **41,** 127–137.

Czechowski, Z., 1994. A kinetic model of the evolution of cracks, *Publs. Inst. Geophys. Pol. Acad. Sci.,* **22,** 262.

Czechowski, Z., 1995. Dynamics of fracturing and cracks, in *Theory of Earthquake Premonitory and Fracture Processes*, pp. 447–469, ed. Teisseyre, R., PWN, Warsaw.

Czechowski, Z., 2001. Transformation of random distributions into power-like distributions due to non-linearities: application to geophysical phenomena, *Geophys. J. Int.,* **144,** 197–205.

Gardiner, C.W., 1985. *Handbook of Stochastic Methods for Physics, Chemistry and the Natural Sciences,* Springer-Verlag, Berlin Heidelberg.

Heimpel, M., 1996. Earthquake size-frequency relations from an analytical stochastic rupture model, *J. geophys. Res.,* **101,** 22 435–22 448.

Hirata, T., 1987. Omori's power law aftershock sequences of microfracturing in rock fracture experiments, *J. geophys. Res.,* **92,** 6215–6221.

Hirata, T., Satoh, T. & Ito, K., 1987. Fractal structure of spatial distribution of microfracturing in rock, *Geophys. J. R. astr. Soc.,* **90,** 369–374.

Ito, K. & Matsuzaki, M., 1990. Earthquakes as self-organized critical phenomena, *J. geophys. Res.,* **95,** 6853–6860.

Klein, W., Rundle, J.B. & Ferguson, C.D., 1997. Scaling and nucleation in models of earthquakes faults, *Phys. Rev. Lett.,* **78,** 3793–3796.

Klein, W., Anghel, M., Ferguson, C.D., Rundle, J.B. & Sa Martins, J.S., 2000. Statistical analysis of a model for earthquake faults with long-range stress transfer, in *GeoComplexity and the Physics of Earthquakes,* pp. 43–71, eds Rundle, J.B., Turcotte, D.L., Klein, W., American Geophysical Union, Washington.

Lomnitz-Adler, J., 1985. The statistical dynamics of the earthquake process, *Bull. seism. Soc. Am.,* **75,** 441–454.

Lomnitz-Adler, J., 1988. The theoretical seismicity of asperity models: an application to the coast of Oaxaca, *Geophys. J.,* **95,** 491–501.

Mogi, K., 1962. Study of elastic shocks caused by the fracture of heterogeneous materials and its relations to earthquake phenomena, *Bull. Earthquake Res. Inst.*, Univ. Tokyo, **40,** 831–853.

Montroll, E.W. & Schlesinger, M.F., 1983. Maximum entropy formalism, fractals, scaling phenomena, and $1/f$ noise: a tale of tails, *J. Statist. Phys.,* **32,** 209–230.

Newman, W., Gabrielov, A., Durand, T., Phoenix, S.L. & Turcotte, D., 1994. An exact renormalization model for earthquakes and material failure: statics and dynamics, *Physica D,* **77,** 200–216.

Olami, Z., Feder, H.J. & Christensen, K., 1992. Self-organized criticality in a continuous, nonconservative cellular automaton modelling earthquakes, *Phys. Rev. Lett.,* **68,** 1244–1247.

Rundle, J.B., Klein, W., Gross, S. & Ferguson, C.D., 1997. The traveling density wave model for earthquake and driven threshold systems, *Phys. Rev. E.,* **56,** 293–302.

Rundle, J.B., Klein, W. & Gross, S., 1999. Physical basis for statistical patterns in complex earthquake populations: models predictions and tests, *Pure appl. Geophys.,* **155,** 575–607.

Rundle, J.B., Klein, W., Turcotte, D. & Malamud, B.D., 2000. Precursory seismic activation and critical-point phenomena, *Pure appl. Geophys.,* **157,** 2165–2182.

Safronov, V.S., 1972. *Evolution of the Protoplanetary Cloud and Formation of the Earth and the Planets,* IPST, Jerusalem.

Sahimi, M., 1995. *Flow and Transport in Porous Media and Fractured Media: from Classical Methods to Modern Approaches,* Weinhein, New York, VCH.

Shaw, B.E. & Rice, J.R., 2000. Existence of continuum complexity in the elastodynamics of repeated fault ruptures, *J. geophys. Res.,* **105,** 23 791–23 810.

Sholz, C.H., 1968. Microfracturing and the inelastic deformation of rock in compression, *J. geophys. Res.,* **73,** 1417–1454.

Sornette, D., Davy, P. & Sornette, A., 1990. Structuration of the lithosphere in plate tectonics as a self-organized phenomenon, *J. geophys. Res.,* **95,** 17 353–17 361.

Stark, H. & Woods, J.W., 1986. *Probability, Random Processes, and Estimation Theory for Engineers,* Prentice-Hall, Englewood Cliffs.

Stauffer, D. & Aharony, A., 1992. *Introduction to Percolation Theory,* Taylor and Francis, London.

Sykes, M.F., Gaunt, D.S., Glen, M. & Ruskin, H., 1981. *J. Phys.*, A, **14,** 287.

Turcotte, D.L., 1992. *Fractals and Chaos in Geology and Geophysics,* Cambridge University Press, Cambridge.

Turcotte, D.L., Newman, W.I. & Gabrielov, A., 2000. A statistical physics approach to earthquakes, in *GeoComplexity and the Physics of Earthquakes*, pp. 83–96, eds Rundle, J.B., Turcotte, D.L. & Klein, W., American Geophysical Union, Washington.

Wu, Z.L., 1998. Implications of a percolation model for earthquake 'nucleation', *Geophys. J. Int.,* **133,** 104–110.

van Kampen, N.G., 1987. *Stochastic Processes in Physics and Chemistry,* North-Holland, Amsterdam.

Vere-Jones, D., 1976. A branching model for crack propagation, *Pageophys.,* **114,** 711–726.